

SIGNIFICANT EFFECT OF GRAPHENE ON CATALYTIC DEGRADATION OF METHYLENE BLUE BY PURE AND Ce-DOPED TiO₂ AT NANOSCALE

Z. ALI^{a,b*}, M. N. CHAUDHRY^a, N. A. NIAZ^c, N. R. KHALID^c,
E. AHMED^c, R. HUSSAIN^d, I. AHMAD^d, S. M. ABBAS^b

^aCollege of Earth & Environmental Sciences, University of the Punjab, Lahore, Pakistan

^bNational Centre for Physics, Quaid-e-Azam University Campus 44000, Islamabad, Pakistan

^cDepartment of Physics, Bahauddin Zakariya University, Multan 60800, Pakistan

^dDepartment of Physics, COMSATS Institute of Information Technology, Islamabad

A novel Ce-TiO₂/graphene composite photocatalyst was synthesized by method of hydrothermal. The synthesized catalysts were analyzed by TEM, XRD, and XPS, DRS and PL spectroscopy, TGA and GC-MS. The results demonstrate that Ce-TiO₂/graphene catalysts showed enhanced absorption of light energy in visible region, also inhibited the recombination of charge carrier due to cooperative effects of graphene and cerium. The photocatalytic action of prepared catalysts was investigated by degradation of dye methylene blue (MB) under solar irradiation. The GC-MS results shows that the dye Methylene Blue has completely mineralized to CO₂ and H₂O. The synthesized composites of Ce-TiO₂/graphene showed enhanced catalytic activity for MB degradation compared to Ce-TiO₂ and pure TiO₂. The improved photocatalytic degradation of MB can be attributed to excellent properties of graphene.

(Received May 7, 2013; Accepted November 1, 2013)

Keywords: TiO₂, Composites, Graphene, Hydrothermal, photocatalysis

1. Introduction

The growth of industry has tremendously increased the generation and accumulation of waste byproducts. Scientists from the whole world have been working on different approaches to address this issue[1]. The photocatalytic degradation of organic compounds has attracted much attention due to its potential to purify wastewater that is discharge from industry and households[2]. The aquatic eco-system is disturbed due to the deficiency of oxygen and light transmission [3]. Titanium dioxide (TiO₂) is considered very close to an ideal semiconductor for photocatalysis because of its high stability, low cost and safety toward both humans and the environment[4]. The limited optical absorption and recombination of photo generated electron-hole pair results in low activity of TiO₂ as photocatalyst[5]. There is an enormous need to improve its activity under solar light by suitable surface modification. Hence more research in future is needed for the development of TiO₂ based materials which are able to capture additional amount of solar energy [6,7]. Therefore many efforts have been employed to improve TiO₂ photocatalytic efficiency, such as doping of metals, code position of noble metals and mixing of two semiconductors[8-12]. Graphene like carbon/TiO₂ show the better photocatalytic activity as compare to pristine TiO₂ (P25) under UV light irradiation[13]. Lanthanide (Ln) doped TiO₂ has drawn much attention due to their 4f electron configuration. Among them cerium doping attracted more interest due to following reasons: (a) the redox coupling Ce⁺³/Ce⁺⁴ makes cerium oxide shift between CeO₂ and CeO₃ under oxidizing and reducing conditions, (b) the different electronic structure between Ce⁺³ (4f⁵5d⁰) and Ce⁺⁴ (4f⁰5d⁰) could result in different optical properties and different catalytic properties[14-16].

*Corresponding author: zali1964@hotmail.com

In addition, the carbonaceous materials have also significant effect on photodegradation due to unique pore structures, electronic configuration and adsorption ability such as CNTs, CNFs and graphene [17]. Monolayer of carbon atoms closely packed in a honeycomb lattice named as graphene, has attracted a great deal of scientific interest due to its unique structure, and electrical, mechanical and optical properties[18]. Therefore it is enviable approach to design graphene based composite for diverse applications. Many efforts have been made to use graphene composite for biosensor, solar cell, to decrease the green house gases effect. The combination of TiO₂ with graphene is also a valuable approach for synthesis of excellent photocatalysis performance. The chemical bonding between TiO₂ and graphene provide spatial condition for charge transport from TiO₂ and graphene via interfaces and then achieved a good catalytic activity[19-22].

In this study, Ce-doped anatase TiO₂ nanoparticles were successfully synthesized and then successfully decorated with graphene oxide layer by hydrothermal method. The synthesized GR-Ce/TiO₂ nanocomposite show tremendous photocatalytic activity and improve the optical properties under visible region than Ce-doped TiO₂ and pure TiO₂ nanoparticles.

2. Materials and Methods

2.1. Synthesis of Cerium-TiO₂/Graphene Composites

First of all hydrothermal method was used for the synthesis of cerium doped TiO₂ catalysts. In the synthesis process, 10 ml of tetra butyl titanate was dissolved in 50 mL ethanol. After that in this solution 25 ml of deionized water at 2.5 pH, (6M HCl) were mixed drop wise under strong stirring. Then a given amount of Ce (NO₃)₃.6H₂O, were mixed in the prepared solution. Then the whole solution was stirred for 30 min duration of time. Here after, the consequential suspension were placed into 100 mL autoclave sealed by Teflon at 170 °C for 12 h. At the end, the mixture was washed by deionized water and then it was centrifuged much time till the pH 7 was obtained. After that, these catalysts were dried out in oven at 120 °C for 12 h. Then these catalysts were calcined at 400 °C to attain Ce doped TiO₂ nanopowder. The elemental composition of Ce to TiO₂ was 0.015% to 0.025%.

The Graphene oxide (GO) from graphite powder (Alfa Aesar 99.99%) was prepared accordingly to the mentioned report[23]. The Ce-TiO₂/graphene catalysts were prepared by method of hydrothermal. For this, 25 mg of graphene oxide dissolved in 40 mL distilled water and 20 mL ethanol followed by ultrasonic treatment for 2 h. After that 250 mg of (TiO₂ or Ce-TiO₂) was added in the solution and strongly stirred for 3 h. Due to which a homogeneous suspension was obtained. After that the suspension was put into autoclave and at 150 °C for 4 h to get the TiO₂/graphene composites. Finally, the resulting composite was obtained by filtration, rinsed by deionized water several times, and then dried at 60 °C for 10 h [24].

2.2 Characterization

The X-ray diffraction (XRD) patterns were obtained by diffractometer (Rigaku D/max-3B X-ray) having Cu K α as a source of radiation ($\lambda=0.15406$ nm) at 40 kV and 36 mA. Transmission electron microscopy (TEM, JEOL JEM-1200EX) was carried out with an accelerating voltage of 200 kV. The X-ray photoelectron spectroscopy (XPS) characterization was performed by (Thermo-VG Scientific, ESCALAB 250) with Al K α as a source of X-ray. All the values of binding energy of XPS spectra were calibrated by taking the reference to the peak of C1s (284.6 eV) arise from adventitious carbon. The most common technique used for analysis of products of dye degraded samples is the coupling of gas chromatography with mass spectrometry GC-MS-QP2010 Ultra Gas Chromatograph Mass Spectrometer SHAMADZU.

The absorption spectra (UV-VIS) were collected under the mode of diffuse reflectance from 300-800 nm range by the use of UV-VIS spectrometer (HITACHI U-4100) with an accessory of integrating sphere. The catalyst powders were used in the form of pellets. These pellets were placed on BaSO₄ plate, used as a standard (reference) for instrumental background correction. The photoluminescence (PL) emission spectra of the samples were obtained by using Fluorescence spectrophotometer (F-4500 Hitachi). For this purpose these samples, excited by light of wavelength of 380 nm at room temperature. The emission was scanned between wavelengths 400 – 700 nm. The photocatalytic activity of the as-prepared catalysts was measured by observing the degradation pattern of methylene blue (MB) dye under solar irradiation at ambient temperature. In

typical reaction, 0.1 g of the synthesized photocatalyst was mixed in 100 mL dye solution (100 ppm) in a beaker. Before illumination, the diverse solution was stirred strongly magnetically for 30 min in the dark to achieve adsorption equilibration. After that the solution was exposed to sunlight for 100 min in a beaker. At a set of exposure time, 3 ml suspension was taken each time. After centrifuged the sample it was taken out for absorption measurement through UV-VIS spectrophotometer. The strength of the major absorption peak (660 nm) of dye methylene blue, referred for the measurement of the remaining concentration (C) of the dye solution.

3. Results and discussion

3.1 X-ray Diffraction

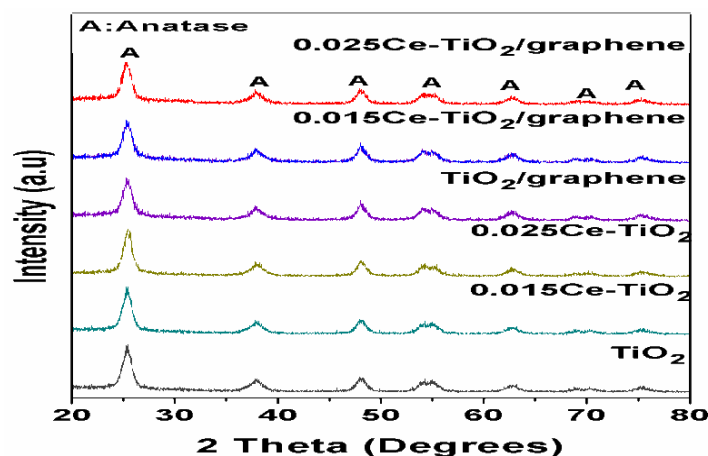


Fig.(1). XRD patterns of synthesized samples.

Fig.(1) shows XRD patterns of undoped, Ce doped TiO_2 , $\text{Ce-TiO}_2/\text{graphene}$ composites clearly showing anatase phase structure of TiO_2 according to (JCPDS-21-1272). No peaks of other than anatase TiO_2 were observed, which confirmed that all doping cerium had been incorporated into TiO_2 crystal structure. It is also noteworthy that the incorporation of graphene did not change the structure of TiO_2 . The crystallite size of the samples were calculated from full-width at half-maxima of the (200) peak of the anatase TiO_2 by Debye-Scherrer according to Equation 1.

$$d = k\lambda / \beta \cos\Theta \quad (1)$$

Where d represents the crystallite size of, λ represents the wavelength of incident X-ray, β is full width at half maximum (FWHM) of diffraction peak and Θ represents the scattering angle. The crystallite size calculated from above equation is 9.0 nm for pure TiO_2 , while the size decreased to 8.0 nm, 7.1 nm for 0.015Ce- TiO_2 and 0.025Ce- TiO_2 samples respectively. It is seen that the crystallite size decreased after doping with cerium. It might be ascribed to the segregation of the doping ions at grain boundary, in turn due to bigger ionic radii of Ce^{+3} (0.111 nm) and Ce^{+4} (0.101 nm) than Ti^{+4} (0.068 nm), where it was difficult for Ce^{+3} and Ce^{+4} to replace Ti^{+4} in the crystalline lattice[25-28]. Therefore, cerium doping might inhibit the growth of crystallite of anatase TiO_2 .

3.2 Transmission Electron Microscopy

Morphological features of the synthesized powders were examined by TEM. Fig. (2a) shows the TEM image of pure TiO_2 nanopowder having particles size in the range of 10 – 15 nm. TEM of 0.15Ce- $\text{TiO}_2/\text{graphene}$ composite demonstrates that TiO_2 nanoparticles were dispersed successfully on the graphene plane Fig. (2b).

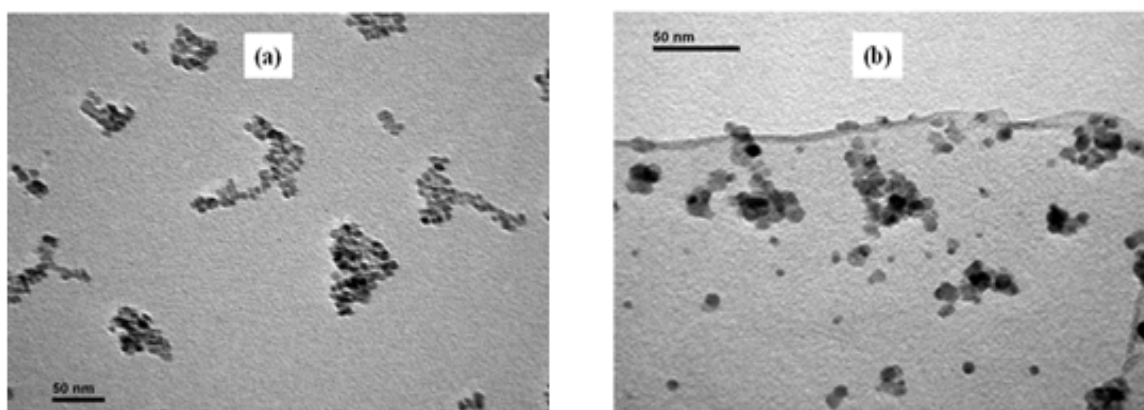


Fig.(2). The TEM images of (a) TiO_2 and (b) $0.15\text{Ce-TiO}_2/\text{graphene}$ composite.

3.3 X-ray Photoelectron Spectroscopy

In order to analyze the chemical composition and purity of the samples, XPS investigation was conducted. Fig. (3) Shows the spectrum of XPS survey $0.015\text{Ce-TiO}_2/\text{graphene}$ composite sample. It clearly shows that sample contains only Ti, O, C and Ce elements. The $\text{Ti}2\text{p}$ core level XPS spectrum Fig.(4) of the prepared sample shows two peaks at 464.7 and 459.0 eV, which are assigned respectively to the $\text{Ti}2\text{p}_{1/2}$ and $\text{Ti}2\text{p}_{3/2}$ spin-orbit splitting photoelectrons in the Ti^{+4} state. [23] In $\text{O}1\text{s}$ core level spectrum Fig. (4), the two peaks at 530.2 and 531.8 eV can be attributed to oxygen lattice and hydroxyl groups respectively[26]. In high-resolution XPS spectrum of $\text{C}1\text{s}$ Fig.(4), the main peak was observed at 284.8 eV, which corresponds the adsorption of adventitious carbon on the surface of sample, the second peak at 285.8 is ascribed to elemental carbon. The peak at 289.2 eV corresponds to $\text{C}=\text{O}$ bonds implying coordinate bonds between Ti and carboxylic acids on the graphene sheets surface. [27] $\text{Ce}3\text{d}$ XPS spectrum Fig. (4) is quite complicated due to hybridization of $\text{Ce}4\text{f}$ and $\text{O}2\text{p}$ electrons, therefore it is fitted to two peaks corresponding to $3\text{d}_{3/2}$ and $3\text{d}_{5/2}$ contributions [28].

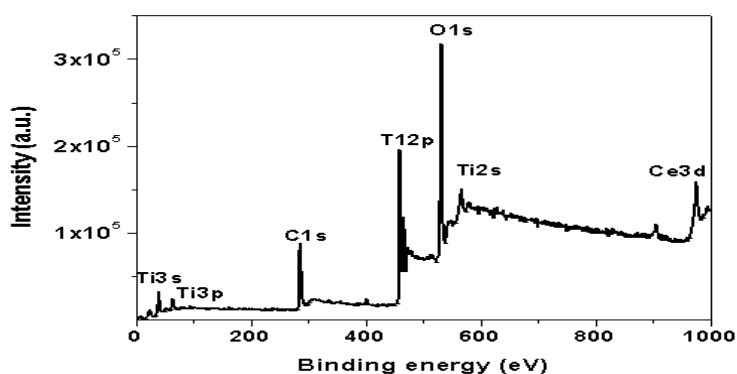


Fig.(3). XPS survey spectrum of $0.015\text{Ce-TiO}_2/\text{graphene}$ composite.

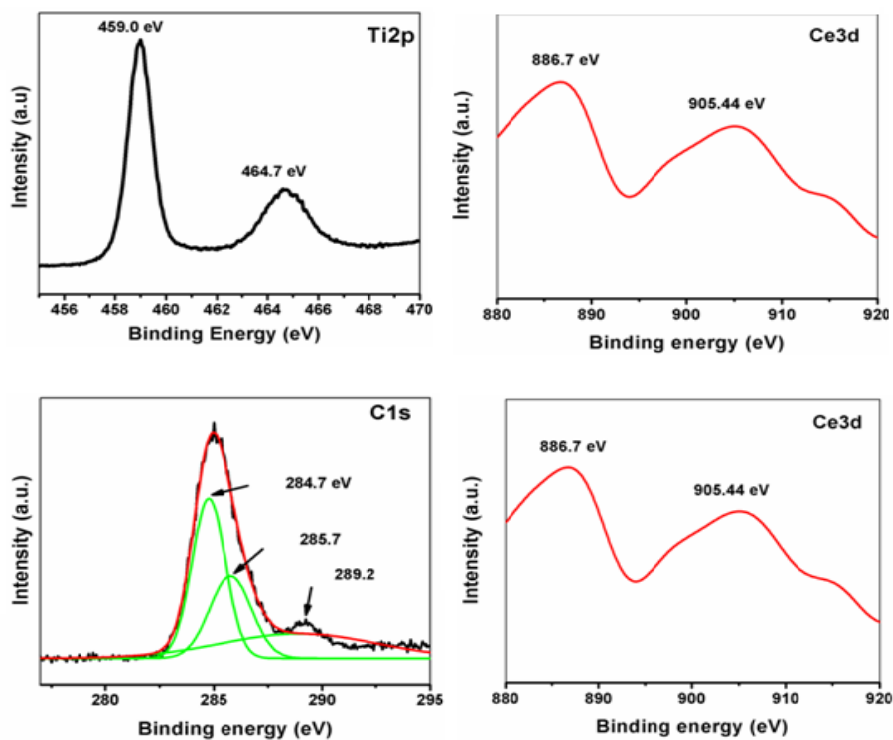


Fig.(4) XPS spectra of Ti2p, O1s and C1s and Ce3d of 0.015Ce-TiO₂/graphene composite.

3.4 Thermogravimetric Analysis

The thermo gravimetric analysis of the synthesized samples 0.015 Ce-TiO₂, 0.025 Ce-TiO₂, TiO₂/graphene, 0.015 Ce-TiO₂/graphene, 0.025 Ce-TiO₂/graphene and pure TiO₂ is shown in Fig. (5). It is obviously seen from TGA results that all samples display continuous weight loss up till 600 °C. The rate of loss of weight up to 160 °C is greater and then up to 600 °C, it becomes slow. The loss of weight up to 160 °C is due to the removal of water adsorbed at the surface of catalyst; whereas the weight losses between 160 °C to 600 °C is due to the interlayer water absorption.

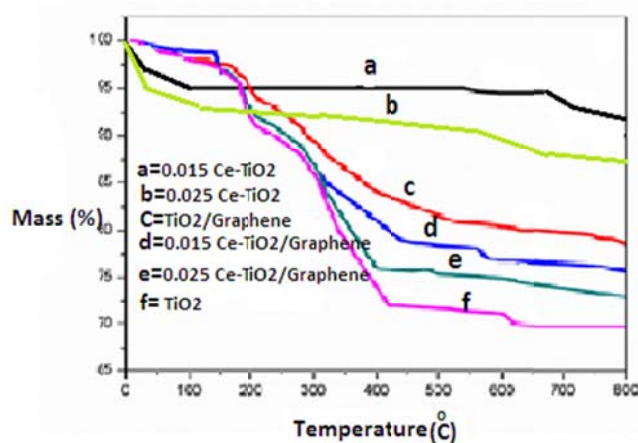


Fig.(5). TGA curve of the synthesized samples.

3.5 UV-VIS Absorption spectra

To investigate the possible change in optical properties of Ce doped TiO₂/graphene composites, the UV-visible absorption spectra of different catalysts were obtained as shown in Fig 6. From these absorption spectra, it is noticeable that pure TiO₂ absorbs at wavelengths shorter

than 400 nm. With the doping of cerium, the absorption edge shifts towards longer wavelengths, thus extending absorption into visible region. The absorption shift in Ce-TiO₂ catalysts can be attributed to the Ce 4f level [25], which has improved the generation of electrons and holes under visible light irradiation. Moreover, graphene introduction into Ce-TiO₂/graphene composites has also shifted the light absorption in visible light region due to excellent optical properties of graphene. The shift of the absorption edge of the Ce-TiO₂/graphene composites can be possibly ascribed to be due to the chemical interaction between TiO₂ and graphene [26, 27].

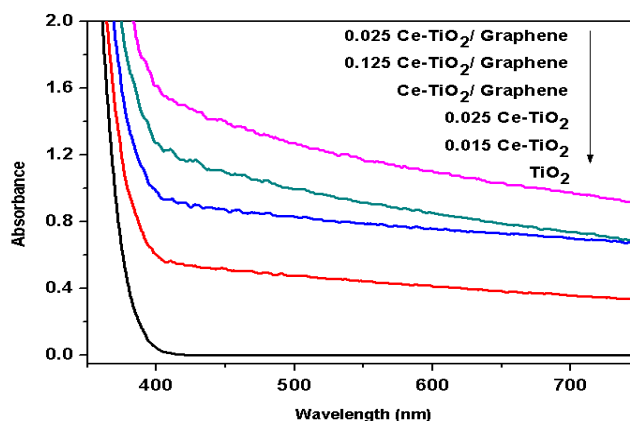


Fig.(6) UV-VIS absorption spectra of different photocatalysts.

3.6 Photoluminescence

The photoluminescence emission spectra techniques have been given a great deal of attention in the field of photocatalysis as a useful probe to understand the surface processes in which photogenerated charge carriers take part [23]. To reveal the effect of Ce doping and graphene incorporation on the photoexcited electron – hole pairs, the PL emission spectra of different samples were examined and results are shown in Fig. (7). It can be seen that doping of cerium and graphene modification reduced the PL emission intensity, showing lower recombination of electron – hole pairs than pure TiO₂. The lowest PL emission intensity was observed for 0.015Ce-TiO₂/graphene composite photocatalyst, which demonstrates that Ce and graphene may act as an electron-trapped agent and thus promote electron separation and transfer processes.

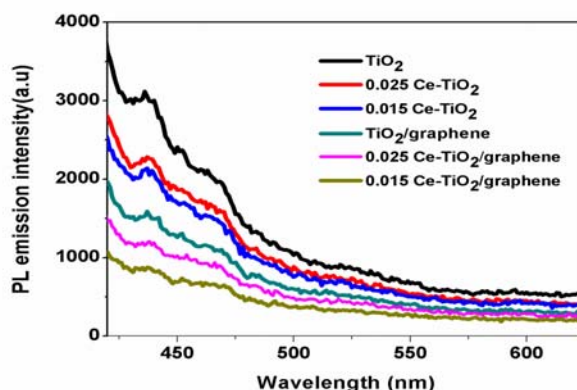


Fig.(7).Photoluminescence spectra of various photocatalysts.

3.7 Gas Chromatography-Mass Spectrometry

The degradation of dye methylene leads to the conversion of organic carbon into risk-free gaseous CO₂ and water. The formation of these risk-free products are reported in Fig. (8) for a

solar irradiation period of 100 min. The gaseous sample was collected in an evacuated cell from Schelling tube and analyzed by GC-MS. It is evident from the GC-MS result Fig. (9) That after the degradation of dye, mainly CO₂ and H₂O was found, showing the complete mineralization of dye [29, 30]. The intermediates produced during the degradation process were analysed by GC/MS and identified according to commercial standards and by the mass spectra through interpretation of their fragment ions.



Fig. (8). Transferring of gaseous mixture from Schelling tube to evacuated reactor.

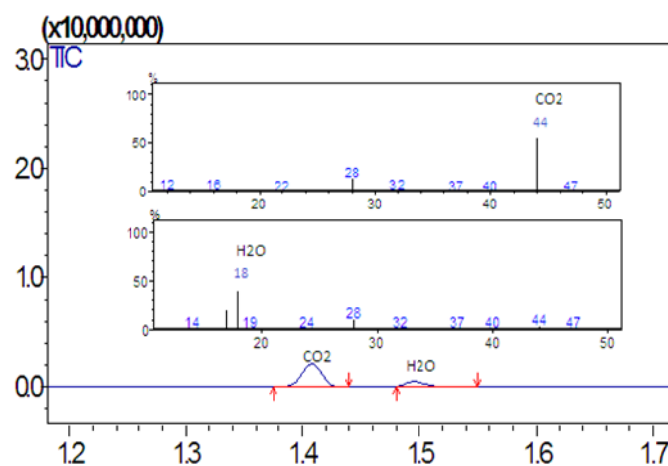


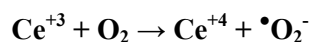
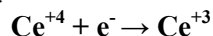
Fig. (9). GC-MS result for mineralization of dye methylene blue

3.8 Photocatalytic Activity of Synthesized Catalysts

Photocatalytic activity of Ce doped TiO₂ and Ce doped TiO₂/graphene composite was evaluated for the degradation of methylene blue under solar light irradiation. A 100 ppm solution of the dye methylene blue was prepared and each time 100 mL solution was taken in a beaker by adding 0.1 g/L of catalyst. A continuous stirring was done under sunlight. To enhance the solar light intensity four reflecting mirror were used. A sample of 3 mL solution was taken after 10 min interval for analysis by UV-Vis Spectrophotometer. Fig. (10) Shows the degradation of methylene blue when different photocatalysts were used. It can be observed that 0.15Ce-TiO₂/Gr catalyst enhanced the photocatalytic performance of TiO₂ as compared to 0.25Ce-TiO₂/Gr and pure TiO₂, which suggests an optimum doping level. A degradation of about 98.5% was found in case of catalyst 0.15/Ce/grapheme as shown in Fig. (11a). Furthermore, the graphene incorporation also enhanced the photocatalytic activity of the catalyst. The photodegradation reaction of methylene blue with the catalysts agrees well with the pseudo-first-order kinetics Fig. (11b). An integrated rate equation is suggested as follows: $\ln(C_0/C) = kt$, where C₀ and C are the initial concentration and concentration at time t of methylene blue and k is apparent degradation rate constant. The rate constants for TiO₂, 0.15Ce-TiO₂, 0.25Ce-TiO₂, 0.15Ce/TiO₂-graphene and 0.25Ce-TiO₂-graphene are 0.007, 0.011, 0.013, 0.018 and 0.024 min⁻¹, respectively. The explanation for the enhanced

photocatalytic activity of the catalysts due to cerium doping and graphene incorporation is elucidated in the following:

Firstly, Ce^{+4} dopants in TiO_2 nanoparticles served as an electron trap in the reaction because of its varied valences and 4f levels [22- 25]. The photo excited electron can be trapped by Ce^{+4} ions through the following process:



Then, the electrons trapped in $\text{Ce}^{+4}/\text{Ce}^{+3}$ sites are transferred to the surrounding adsorbed oxygen. Therefore, the recombination of electron-hole pairs is largely prevented, resulting in an increase in the photocatalytic activity of Ce doped TiO_2 nanoparticles. Secondly, due to two-dimensional π -conjugation structure, graphene can act as an electron acceptor, thereby allowing the photo generated electrons of TiO_2 in the composite to be quickly transferred from the conduction band of TiO_2 to graphene [26, 27]. This eventually reduces the rate of recombination of electron – hole pairs, which results in an enhanced photocatalytic performance of the composites.

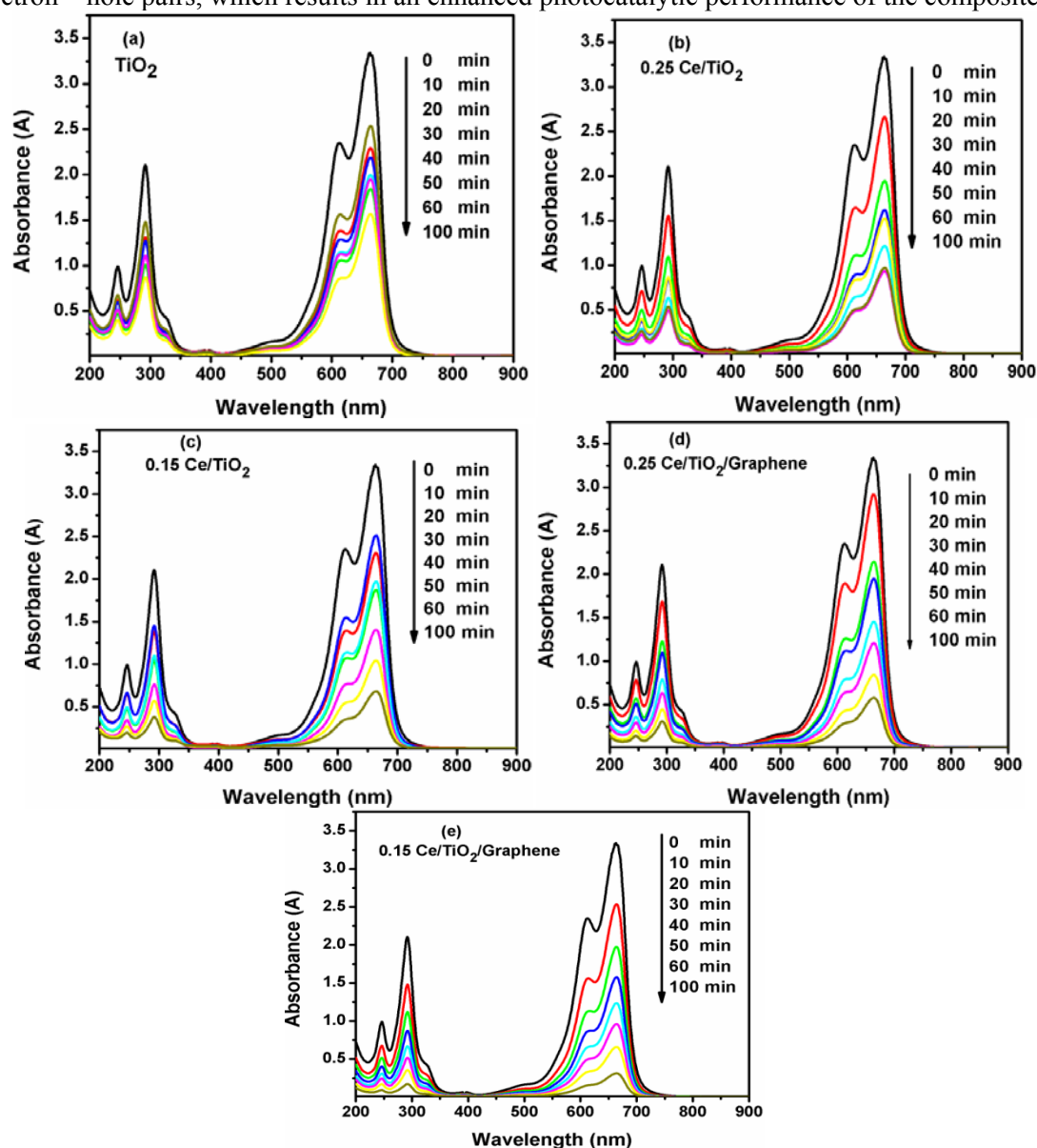


Fig. (10). UV-Vis spectral variations of Methylene Blue aqueous solution (100ppm) during solar irradiation by Catalyst (a) TiO_2 , (b) 0.25 Ce/TiO_2 , (c) 0.15 Ce/TiO_2 , (d) $0.25 \text{ Ce/TiO}_2/\text{Graphene}$ (e) $0.15 \text{ Ce/TiO}_2/\text{Graphene}$

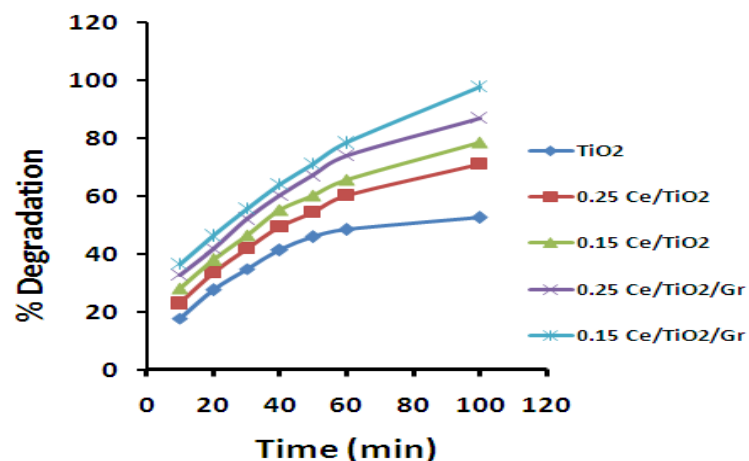


Fig. (11a). Percentage degradation of methylene blue with the increase in solar-irradiation time.

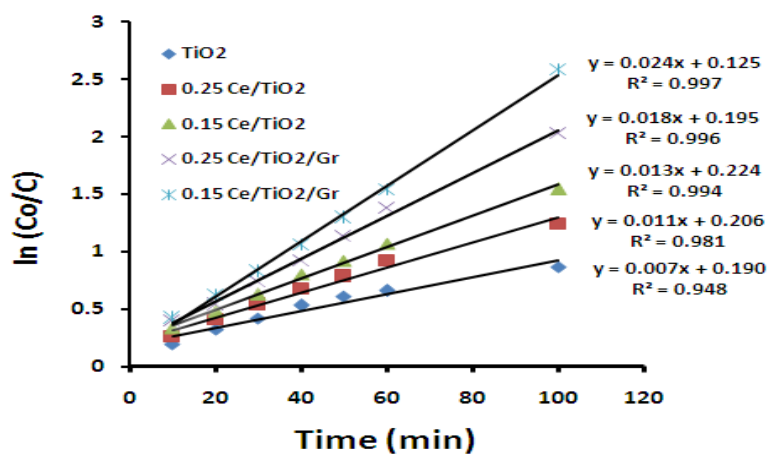


Fig. (11b). A plot of $\ln(Co/C)$ versus solar irradiation time for an aqueous solution of methylene blue (10 mgL^{-1}) and curve fit data for the first order degradation kinetics

4. Conclusion

Ce-TiO₂ photocatalysts were successfully synthesized by hydrothermal method. From them a better photocatalytic activity of cerium doped TiO₂/graphene composites could be attributed to synergy effects including enhanced visible light absorption, improved charge carriers separation as well as to the formation of $\pi - \pi$ conjugation structure of graphene sheets. Both the cerium doping and graphene modification are promising ways to achieve cheap and efficient photocatalysts for visible light activation.

Acknowledgement

I would like to acknowledge and extend my heartfelt gratitude to the persons who helped me for this research work. I also acknowledge Nano Science & Catalysis Division, National Centre for Physics, Quaid-i-Azam University Islamabad.

References

- [1] A. Mills, S. Le Hunte, J. Photochem. Photobiol. A. **108**, 1 (1997).
- [2] D. Zhao, Xin Yang, Changlun Chen, Xiangke Wang, J. of Colloid & Interface Science. **398**, 234 (2013).
- [3] A. Zulfiqar, M.N. Chaudhry, S.T. Hussain, S. A. Batool, S. M. Abbas, N. Ahmad, N. Ali, N.A. Niaz, Digest Journal of Nanomaterials and Biostructures **8**(3), 1271 (2013).
- [4] K. Hashimoto, I. Hiroshi and A. Fujishima, Jap. J. of Appl. Phys., **44**, 8269 (2005).
- [5] N.R. Khalid, E. Ahmed, Zhanglian Hong, Yüewei Zhang, M. Ahmad, Curr. Appl. Phys. xxx 1-8 (2012).
- [6] A. Zulfiqar,; M. Aslam,; M. Iqbal,; I. Ismail,; A. Hameed,; S. T. Hussain,; M. N. Chaudhry,; M. A. Gondal, Journal of Environmental Science and Health, Part **A49**, 125 (2014)
- [7] A. Zulfiqar, S. T. Hussain, M. N. Chaudhry, S. A. Batool, T. Mahmood, International Journal of Physical Sciences. **8**(22), 1201 (2013).
- [8] R. Asahi, T. Morikawa, T. Ohwaki, K. Aoki, Y. Taga, Science, **293**, 4943 (2001).
- [9] B. Krautler. A.J. Bard. J. Am. Chem. Soc. **100**, 4317 (1978).
- [10] V. Subramanian, E.E. Wolf, P. V. Kamat, J. Am. Chem. Soc. **126**, 4943 (2004).
- [11] H. G. Kim, P. H. Bors, W. Choi, J. S. Lee, angew. Chem. Int. Ed. **44**, 4585 (2005).
- [12] X. Fu, L. A. Clark, Q. Yang, M. A. Anderson, Environ. Science Tech. **30**, 647 (1996).
- [13] W. Yajun, S. Rui, L. Jei, Z. Yongfa, Appl. Cataly. B: Environ. **100**, 179 (2010).
- [14] F. B. Li, X.X. Li, M. F. Hou, K.W. Cheah, W.C.H. Choy, Appl. Cataly. A, **285**, 181 (2005).
- [15] A. M. T. Silva, C.G. Silva, G. Drazic, J.L. Faria, Cataly. Tod. **144**, 13 (2009).
- [16] Y.H. Xu, H.R. Chen, Z. X. Zeng, B. Lei, Appl. Surf. Sci., **252**, 8565 (2006).
- [17] C. Basheer, Journal of Chem. 1-10 (2013).
- [18] Peigney, A. Luarent, C. Flahaut, E. Bacsá, R.R. Rousset, Carbon, **39**, 507 (2001).
- [19] S. Girish Kumar, L. Gomathi Devi J. Phys. Chem. A, **115**, 13211 (2011).
- [20] A. L. Linsebigler, G. Lu, J. T. Yates, Jr. Chem. Rev. **95**, 735 (1995).
- [21] A. T. Vu, Q. T. Nguyen, T. H. Linh Bui, M. C. Tran, T. P. Dang, T. K. Hoa Tran, Adv. Nat. Sci.: Nanosci. Nanotech. **1**, 015009 (2010).
- [22] C-Y. Tsai, H-C.Hsi, T-H.Kuo, Y-M. Chang, J-H Liou, Aero. & Air Qual. Res., **13**, 639 (2013).
- [23] N.R. Khalid, Z. Hong, E. Ahmed, Y. Zhang, H. Chan, M. Ahmad, Appl. Surf. Sci. **258**, 5827 (2012).
- [24] N.R. Khalid,; E. Ahmed,; Z. Hong,; M. Ahmad, Appl. Surf. Sci., **263**, 254-259 (2012).
- [25] J. Xie, D. Jiang, M. Chen, D. Li, J. Zhua, X. Lü, C. Yan, Coll. and Surf. A: Physicochem. Eng. Asp., **372**, 107 (2010).
- [26] M.S.A.S. Shah, A.R. Park, K. Zhang, J.H. Park, P.J. Yoo, Appl. Mater. Interf. **4**, 3893 (2012).
- [27] V. Stengl, S. Bakardjieva, T.M. Grygar, J. Bludska, M. Kormunda, Chem. Central J. **7**, 41 (2013).
- [28] J. Xu, Y. Ao, D. Fu, Appl. Surf. Sci., **256**, 884 (2009).
- [29] M.A. Rauf,; S.A. Salman, Chemical Engineering Journal. **151**, 10 (2009).
- [30] S. T. Hussain,; A. Siddiq, Int. J. Environ. Sci. Tech., **8**(2), 351 (2011)